

Far-infrared photo-conductivity of electrons in an array of nano-structured antidots

K. Bittkau, Ch. Menk, Ch. Heyn, D. Heitmann, and C. -M. Hu*
*Institut für Angewandte Physik und Zentrum für Mikrostrukturforschung,
 Universität Hamburg, Jungiusstraße 11, 20355 Hamburg, Germany*
 (Dated: July 26, 2018)

We present far-infrared (FIR) photo-conductivity measurements for a two-dimensional electron gas in an array of nano-structured antidots. We detect, resistively and spectrally resolved, both the magnetoplasmon and the edge-magnetoplasmon modes. Temperature-dependent measurements demonstrates that both modes contribute to the photo resistance by heating the electron gas via resonant absorption of the FIR radiation. Influences of spin effect and phonon bands on the collective excitations in the antidot lattice are observed.

PACS numbers: 73.43.Lp, 73.50.Pz, 78.67.Hc

There has been recently growing interest to investigate the photo resistance related with the elementary excitations of a two-dimensional electron gas (2DEG) in semiconductor heterostructures^{1,2,3,4,5,6}. For example, under GHz radiation, the magneto-resistance of a 2DEG shows an unexpected large oscillation whose period is determined by the electron cyclotron resonance (CR)¹. Using THz radiation, plasmon of tunneling coupled bilayer 2DEGs is found to contribute to the photo resistance in a unique way⁴. Even the spin effects result in striking photo resistance changes^{2,3}. Among others, the spin-orbit interaction, which was about 80 years ago discovered by the atomic spectroscopy and gave birth to the very concept of *spin*, has been found rather difficult to be spectrally measured for the 2DEGs. The problem has been recently solved by measuring the spin-flip excitation using the photo-conductivity spectroscopy². Of particular interest is the high sensitivity of photo-conductivity technique, which has the potential to study unique elementary electronic excitations of nano-structured semiconductors with only few units. As a first step, very recently Jager *et al.*⁵ and Ye *et al.*⁶ both studied the photo conductivity of a 2DEG in an antidot array. While these nice experiments together with the pioneer one of Vasiliadou *et al.*⁷ have shed light on the interesting photo conductivity effect of a 2DEG in an antidot array, primary questions like the role of the characteristic excitations of the antidot array on its photo resistance are surprisingly left open, which is the central subject of this work.

The elementary electronic excitations of a 2DEG in an antidot array subjected to a perpendicular magnetic field B are dominated by a characteristic two-mode behavior with collective excitations^{8,9}. The upper mode ω^+ approaches at large B field the CR frequency $\omega_c = eB/m^*$, which is determined by the electron effective mass m^* . The lower one ω_{EMP} , known as the edge-magnetoplasmon (EMP) mode, is associated with the electrons skipping around the depleted area with a radius R formed by the antidot potential. Using the modified-

dipole and effective-medium approximations, the dispersion of these modes can be described by⁸

$$1 - \frac{(1-f)\omega_0^2}{\omega(\omega + \omega_c)} - \frac{f\omega_0^2}{\omega(\omega - \omega_c)} = 0. \quad (1)$$

Here ω_0 is the frequency of the ω^+ mode at $B = 0$, depending on the antidot lattice period a , the 2DEG's carrier density N_s , and its dielectric surrounding. The geometrical filling factor $f = \pi R^2/a^2$ indicates the portion of the 2D area where the electrons are depleted. These modes have been well studied by far-infrared (FIR) transmission spectroscopy⁹, but have not been clearly identified in photo-conductivity experiments^{5,6,7}, leaving the question open whether and how they might influence the photo resistance of the 2DEG in an antidot array.

In this rapid communication, we report FIR photo-conductivity experimental results obtained for a 2DEG in an antidot array. We find clearly that both the ω^+ and ω_{EMP} modes contribute to the photo resistance by heating the electron gas via resonant absorption of the FIR radiation. In addition, we present interesting results indicating the influences of spin and electron-phonon interaction in the antidot lattice.

Our sample is an inverted-doped InAs step quantum well with 40 nm $\text{In}_{0.75}\text{Al}_{0.25}\text{As}$ cap layer. The step quantum well is composed of 13.5 nm $\text{In}_{0.75}\text{Ga}_{0.25}\text{As}$, an inserted 4 nm InAs channel, and a 2.5-nm-thick $\text{In}_{0.75}\text{Ga}_{0.25}\text{As}$ layer. Underneath the quantum well is a 5 nm spacer layer of $\text{In}_{0.75}\text{Al}_{0.25}\text{As}$ on top of a 7-nm-wide Si-doped $\text{In}_{0.75}\text{Al}_{0.25}\text{As}$ layer. The sample is grown by molecular beam epitaxy on a buffering multilayer accommodating the lattice mismatch to the semi-insulating GaAs substrate. A self-consistent Schrödinger-Poisson calculation shows that the 2DEG is about 55 nm below the surface, mainly confined in the narrow InAs channel¹⁰. Figure 1 shows a sketch of our sample with antidots. An extreme long 2DEG Hall bar with a channel width of $W = 40 \mu\text{m}$ and a total length L of about 10 cm was defined by chemical wet etching, which contains the antidot array with a period of $a = 800 \text{ nm}$. The holes with a geometric diameter of about 200 nm were defined by holography and chemical wet etching. The 2DEG channel runs meandering in a square of 4×4

*Corresponding author. Email: hu@physnet.uni-hamburg.de

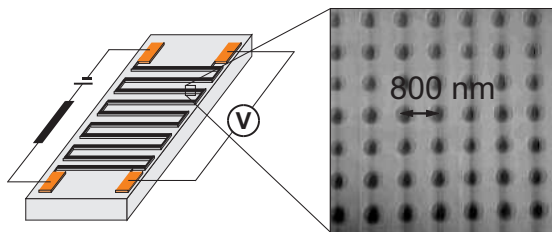


FIG. 1: Schematic bias circuit and sample structure showing the long Hall bar with ohmic contacts. The zoom-in part is an atomic force micrograph of the antidot array.

mm². The extremely large L/W ratio enhances the sensitivity of our measurement. With the antidots, the carrier density N_s and mobility μ at 1.5 K were determined by Shubnikov-de Haas measurement to be $6.01 \times 10^{11} \text{ cm}^{-2}$ and $62\,000 \text{ cm}^2/\text{Vs}$, respectively, reduced compared with those of the corresponding unpatterned sample² of $6.66 \times 10^{11} \text{ cm}^{-2}$ and $150\,000 \text{ cm}^2/\text{Vs}$. Ohmic contacts were made by depositing AuGe alloy followed by annealing.

Our experiment was performed by applying a DC current of $9 \mu\text{A}$ to the Hall bar and measuring the changes of the voltage drop caused by FIR radiation. At fixed magnetic fields, the broadband FIR radiation was modulated by the Michelson interferometer of a Fourier transform spectrometer. Using the sample itself as the detector, the corresponding change in the voltage drop of the sample was AC coupled to a broadband preamplifier and recorded as an interferogram, which was Fourier transformed to get the photo-conductivity spectrum. The sample was mounted in a He cryostat with a superconducting solenoid. All data reported here were obtained in Faraday geometry.

Figure 2 shows typical FIR photo-conductivity spectra measured at different B fields and temperatures. Different beam splitters of the spectrometer are used to optimize the measurement for resonances lying in different frequency regimes. As shown in Fig. 2(a) at the low magnetic field of $B = 3.2 \text{ T}$, two resonances are clearly observed. By increasing the B field to 6.4 T , the resonance at the lower energy has a slight red shift and gets weaker, while the higher-energy resonance shows a significant blue shift and dominates the spectrum. Two additional weak resonances are observed, one appears as a shoulder of the dominant resonance and the other lies at about 285 cm^{-1} , which are indicated by a thick and thin arrow, respectively. By further increasing the B field to 9.6 T , the dominant resonance splits into multi-peaks, while the weak one at 285 cm^{-1} gains resonance strength. The resonance at the low energy disappears at large B fields. In Fig. 2(b) we plot the spectra measured at $B = 3.2 \text{ T}$ and at different temperatures. In this case the DC current was reduced to 180 nA to avoid heating the 2DEG by the current. The observed resonances are found extremely temperature sensitive, with their amplitudes decreasing quickly by only slightly increasing the

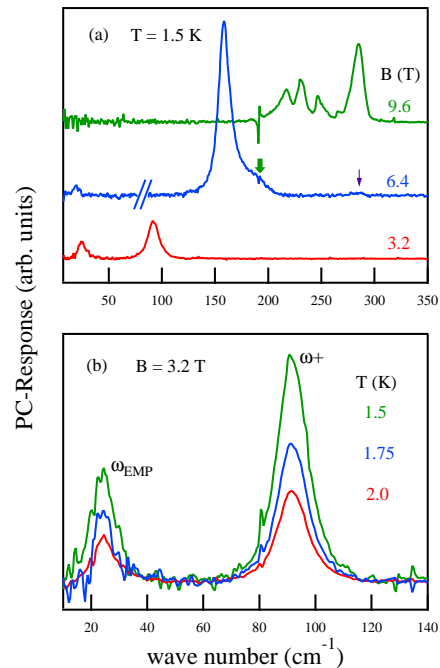


FIG. 2: (color online). FIR photo-conductivity spectra measured at (a) $T = 1.5 \text{ K}$ for three different magnetic fields and (b) $B = 3.2 \text{ T}$ for three different temperatures. Arrows indicate weak resonances described in the text. Spectra in (a) are vertically offset for clarity.

temperature.

In Fig. 3(a) we plot the B -field dispersion of these resonances. Also shown is the magnetoresistance R_{xx} measured without FIR radiation using the standard lock-in technique, which allows us to determine the 2DEG filling factors $\nu = N_s h / eB$. The major resonances can be nicely fit (solid curves) using eq. (1) with three fitting parameters $\omega_0 = 70.2 \text{ cm}^{-1}$, $f = 0.17$, and $m^* = 0.039 m_e$. Within the fitting accuracy, the obtained effective mass value is equal to that directly measured from CR on the unpatterned sample from the same wafer². We therefore identify them as the two characteristic antidot collective modes ω^+ and ω_{EMP} . The relative strength of ω^+ over ω_{EMP} mode increases with increasing B field, in accordance with the theory⁸. By comparing the spectra with that obtained on the unpatterned sample, we further identify the weak resonance marked by the thick arrow in Fig. 2(a) as the collective spin-flip excitation². With the antidot lattice, the collective spin-flip excitation gets broader and appears as a shoulder of the ω^+ resonance. Spin-flip excitation in an antidot array has neither been studied experimentally nor been theoretically investigated. Here we have assumed that at large B fields, the spin-flip excitation in the antidot array approaches that in an unpatterned 2DEG, just like the ω^+ mode approaches the CR⁸. For comparison, we plot in Fig. 3(a) the calculated dispersion for the 2DEG spin-flip excita-

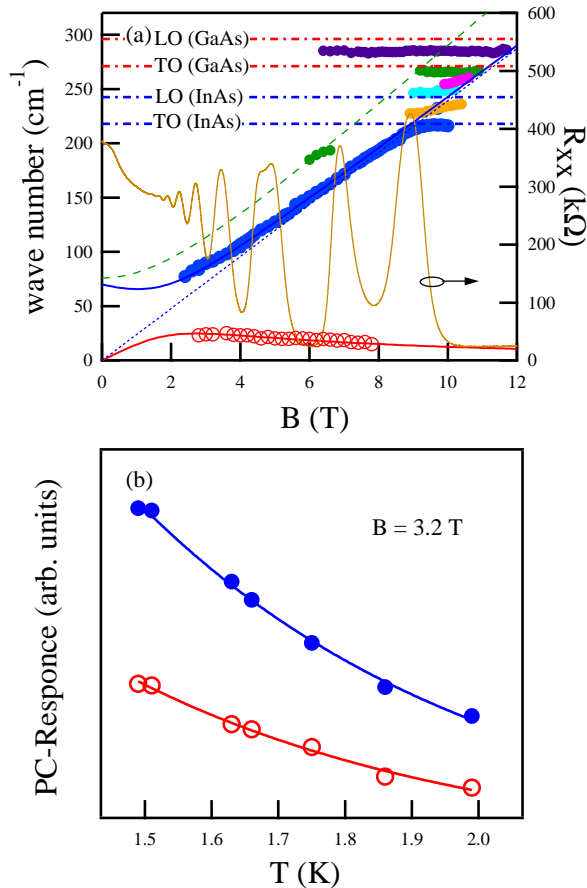


FIG. 3: (color online). (a) Magnetic-field dispersions for resonances measured at $T = 1.5$ K and magnetoresistance R_{xx} measured without FIR radiation. The solid curves are fits for ω^+ (solid circles) and ω_{EMP} (open circles) antidot modes using Eq. (1). The dotted line and dashed curve are calculated for CR and spin-flip excitation, respectively, using the effective mass of $0.039 m_e$, the spin-orbit coupling parameter of $\alpha = 2.38 \times 10^{-11}$ eVm and a Landé g -factor of $g = -8.7$. Dash-dotted lines indicate the optical phonon energies of InAs and GaAs. (b) Temperature dependence of the resonance strength for the ω^+ (solid circles) and ω_{EMP} (open circles) antidot modes measured at $B = 3.2$ T. The curves in (b) are guide to eyes.

tion neglecting both the many-body correction and the antidot potential, using the spin-orbit coupling parameter of $\alpha = 2.38 \times 10^{-11}$ eVm and the Landé g -factor of $g = -8.7$ determined for the unpatterned sample². Within the B -field range of 6 to 7 T where we can observe the spin-flip excitation, influence of the antidot potential on its resonance frequency is found small.

Observing the spin-flip excitation in the antidot lattice demonstrates the high sensitivity advantage of the photo-conductivity spectroscopy. Another advantage of the technique is that we can measure resonances within the reststrahlen bands which are prohibited for transmission spectroscopy. In our sample, both the InAs quantum well and the GaAs substrate are polar semiconduc-

tors with reststrahlen bands between their TO and LO phonon frequencies. Besides, there are two phonon bands for both $\text{In}_{0.75}\text{Ga}_{0.25}\text{As}$ and $\text{In}_{0.75}\text{Al}_{0.25}\text{As}$ layers, as well as the interface phonons near each interfaces. For brevity, we plot in Fig. 3(a) the bulk phonon frequency of GaAs and InAs. Apparently, the splitting of the ω^+ mode at large B fields is caused by the influence of phonons of our sample. Experimentally, by increasing the B field, we find that the resonance at about 285 cm^{-1} indicated by the thin arrow in Fig. 2(a) stays within the reststrahlen band of GaAs substrate but gains resonance strength. While the splitting of the ω^+ mode shows anti-crossing behavior centered at about 220 and 240 cm^{-1} , near the TO (218 cm^{-1}) and LO (242.5 cm^{-1}) phonon frequency of InAs, respectively. At the moment, we cannot explain these resonances in the reststrahlen bands regime. We note that the influence of phonons on electronic excitations of a nano-structured 2DEG in the reststrahlen band regime is a rather sophisticated problem, with the combined nature of the optical effect¹¹, band nonparabolicity, electron-electron and electron-phonon interaction^{12,13}. It remains a controversial subject¹⁴. However, the rich spectral features observed in our experiment provide systematic data that is essential to establish a clear theoretical picture.

Our data demonstrates clearly that both ω^+ and ω_{EMP} antidot modes contribute to the photo resistance. In contrast to that studied by the transmission spectroscopy, the resonance strengths of both modes measured by photo-conductivity spectroscopy are extremely temperature sensitive. As shown in Fig. 2(b) the resonance strengths of both modes decrease quickly by increasing the temperature from 1.5 to 2 K, during which the half width of the resonances does not change much. In Fig. 3(b), we plot the temperature dependence of the resonance strength for both modes measured at $B = 3.2$ T. Such an extremely sensitive temperature dependence can be qualitatively explained by the bolometric effect^{3,15}, where the resonant absorption of the FIR radiation effectively heats the electron gas and hence changes its resistance. In the low temperature limit $k_B T \ll E_F$, the heat capacity of the 2DEG is given by¹⁶

$$C_e = \pi^2 k_B^2 T \mathcal{D}(E_F, B) / 3, \quad (2)$$

proportional to the temperature T and the density of states $\mathcal{D}(E_F, B)$ of the 2DEG at the Fermi energy E_F . Bolometric effect caused by electron heating is therefore more pronounced at lower temperature where C_e is smaller.

It is intriguing to compare our results with other photo-conductivity experiments on the 2DEG in an antidot array. In the early work of Vasiliadou *et al.*⁷, instead of a broad band FIR source, microwave generator was used to investigate the commensurability effects. Photo-conductivity experiment was performed by fixing the microwave frequency while sweeping the magnetic field. Characteristic dispersions for the antidot collective modes were not investigated due to the limited available

microwave frequencies. And temperature dependence was not easy to be studied because of the superposed nonresonant background which originates from heating of the whole sample. In an improved photo-conductivity spectroscopy experiment recently performed by Jager *et al.*⁵, the 2DEG is at a distance of 37 nm below the sample surface and the antidots are written by *e*-beam lithography and transferred into the 2DEG by shallow (with only about 6 nm) wet etching. Therefore, instead of ω^+ and ω_{EMP} modes, CR and a magnetoplasmon mode were simultaneously observed, which is typical for a weak modulated 2DEG instead of the 2DEG with antidot confinement. The most recent experiment was performed by Ye *et al.*⁶ using a significantly improved microwave technique with transmission lines to study both the photo-conductivity and microwave transmission of a 2DEG in an antidot array. Among other interesting results, they observed a broad peak below Landau filling one in the microwave conductivity measured by sweeping the *B* field. On the peak, unlike the DC-limit conductivity, the microwave conductivity was found extremely temperature sensitive, decreasing with increasing temperature. As the possible origins, antidot edge excitations of fractional quantum Hall effect states associated with either the chiral Luttinger liquids⁶ or edge reconstruction¹⁷ have been discussed. Our data provides additional insight. As shown in Fig. 3(b), we have demonstrated that the contribution of the antidot edge-magnetoplasmon to the photo resistance has similar sensitive temperature dependence due to its bolometric nature. Besides, based on the flat *B*-field dispersion of the edge-magnetoplasmon shown in Fig. 3(a), photo resistance caused by exciting the edge-

magnetoplasmon at a fixed frequency would show broad structures, superposed by nonresonant background due to the change of the photo-conductivity sensitivity by sweeping the *B* field. However, we would like to emphasize that whether the edge-magnetoplasmon indeed plays a role in the nice experiment of Ye *et al.*⁶ depends on two major questions: the first one is how does the photo resistance influence the microwave transmission in their experiment; and the second one is how large is the edge-magnetoplasmon frequency in their sample. We note that while the first question is not easy to answer due to the complicated microwave technique. The second question can be clarified by performing photo-conductivity spectroscopy experiment as we describe in this paper. By measuring the dispersion of the ω^+ mode in the FIR regime, the geometric filling factor *f* that depends on the depletion area of the antidot can be determined, which can be used to estimate the ω_{EMP} mode frequency¹⁸. In the sample of Ye *et al.*⁶ the later lies in the microwave regime and is rather difficult to be directly measured.

In summary, we have performed FIR photo-conductivity spectroscopy experiment on a 2DEG in an array of antidot. We find that both the magnetoplasmon (ω^+) and the edge-magnetoplasmon (ω_{EMP}) modes of the antidot contribute to the photo resistance, which is extremely temperature sensitive due to the bolometric nature. We observe the influence of phonon bands on the ω^+ mode and a spin-flip excitation mode in the antidots.

This work is supported by the BMBF through project 01BM905 and the DFG through SFB 508. We thank Axel Lorke and Peide Ye for helpful discussions about the experiments of ref. 5 and 6, respectively.

-
- ¹ M.A. Zudov, R.R. Du, J.A. Simmons, and J.L. Reno, Phys. Rev. B **64**, 201311(R) (2001); R.G. Mani, J.H. Smet, K. von Klitzing, V. Narayanamurti, W.B. Johnson, and V. Umansky, Nature **420**, 646 (2002); M.A. Zudov, R.R. Du, L.N. Pfeiffer, and K.W. West, Phys. Rev. Lett. **90**, 046807(2003).
- ² C.-M. Hu, C. Zehnder, Ch. Heyn, and D. Heitmann, Phys. Rev. B **67**, 201302(R) (2003).
- ³ C. Zehnder, A. Wirthmann, Ch. Heyn, D. Heitmann, and C.-M. Hu, Europhys. Lett., to be published.
- ⁴ X.G. Peralta, S.J. Allen, M.C. Wanke, N.E. Harff, J.A. Simmons, M.P. Lilly, J.L. Reno, P.J. Burke, and J.P. Eisenstein, Appl. Phys. Lett. **81**, 1627 (2002).
- ⁵ B.G.L. Jager, S. Wimmer, A. Lorke, J.P. Kotthaus, W. Wegscheider, and M. Bichler, Phys. Rev. B **63**, 045315 (2001).
- ⁶ P.D. Ye, L.W. Engel, D.C. Tsui, J.A. Simmons, J.R. Wendt, G.A. Vawter, and J.L. Reno, Appl. Phys. Lett. **79**, 2193 (2001); Phys. Rev. B **65**, 121305(R) (2002).
- ⁷ E. Vasiliadou, R. Fleischmann, D. Weiss, D. Heitmann, K. v. Klitzing, T. Geisel, R. Bergmann, H. Schweizer, and C.T. Foxon, Phys. Rev. B **52**, R8658 (1995).
- ⁸ S.A. Mikhailov, and V.A. Volkov, Phys. Rev. B **52**, 17260 (1995); S.A. Mikhailov, Phys. Rev. B **54**, 14293 (1996).
- ⁹ K. Kern, D. Heitmann, P. Grambow, Y. H. Zhang and K. Ploog, Phys. Rev. Lett. **66**, 1618 (1991); A. Lorke, J. P. Kotthaus and K. Ploog, Superlattices and Microstruct. **9**, 103 (1991); Y. Zhao, D. C. Tsui, M. Santos, M. Shayegan, R. A. Ghanbari, D. A. Antoniadis and H. I. Smith, Appl. Phys. Lett. **60**, 1510 (1992).
- ¹⁰ A. Richter, M. Koch, T. Matsuyama, Ch. Heyn, and U. Merkt, Appl. Phys. Lett. **77**, 3227 (2000).
- ¹¹ M. Ziesmann, D. Heitmann, and L. L. Chang, Phys. Rev. B **35**, 4541 (1987).
- ¹² C.-M. Hu, E. Batke, K. Köhler, and P. Ganser, Phys. Rev. Lett. **75**, 918 (1995); Phys. Rev. Lett. **76**, 1904 (1996).
- ¹³ X. G. Wu, F. M. Peeters, Y. J. Wang, and B. D. McCombe, Phys. Rev. Lett. **84**, 4934 (2000).
- ¹⁴ A. J. L. Poulter, J. Zeman, D. K. Maude, M. Potemski, G. Martinez, A. Riedel, R. Hey, and K. J. Friedland, Phys. Rev. Lett. **86**, 336 (2001); Bo Zhang, M. F. Manger, and E. Batke, Phys. Rev. Lett. **89**, 039703 (2002).
- ¹⁵ F. Neppel, J.P. Kotthaus, and J.F. Koch, Phys. Rev. B **19**, 5240 (1979); K. Hirakawa, K. Yamanaka, Y. Kawaguchi, M. Endo, M. Saeki, and S. Komiyama, Phys. Rev. B **63**, 085320 (2001).
- ¹⁶ J.K. Wang, D.C. Tsui, M. Santos, and M. Shayegan, Phys. Rev. B **45**, 4384 (1992).

¹⁷ X. Wan, K. Yang, and E.H. Rezayi, Phys. Rev. Lett. **88**, 056802 (2002).

¹⁸ One might need also estimating the half width of the ω_{EMP} mode (of the order of 100 GHz in our sample), since excit-

ing the tail of the ω_{EMP} mode could also cause a B -field dependent photo resistance.